# Multiple periods of functional ocular dominance plasticity in mouse visual cortex

Yoshiaki Tagawa[1,2,3], Patrick O Kanold[1,3], Marta Majdan[1] & Carla J Shatz[1]

The precise period when experience shapes neural circuits in the mouse visual system is unknown. We used Arc induction to monitor the functional pattern of ipsilateral eye representation in cortex during normal development and after visual deprivation. After monocular deprivation during the critical period, Arc induction reflects ocular dominance (OD) shifts within the binocular zone. Arc induction also reports faithfully expected OD shifts in cat. Shifts towards the open eye and weakening of the deprived eye were seen in layer 4 after the critical period ends and also before it begins. These shifts include an unexpected spatial expansion of Arc induction into the monocular zone. However, this plasticity is not present in adult layer 6. Thus, functionally assessed OD can be altered in cortex by ocular imbalances substantially earlier and far later than expected.

Sensory experience can modify structural and functional connectivity in cortex[1,2]. Many previous studies of highly binocular animals have led to the current consensus that visual experience is required for maintenance of precise connections in the developing visual cortex and that competition-based mechanisms underlie ocular dominance (OD) plasticity during a critical period[3–6]. To elucidate cellular and molecular mechanisms underlying the critical period, recent experiments have used mouse visual system as a model[6–9]. In mouse, retinal projections to the LGN are almost completely crossed. Consequently, visual cortex contains a large monocular zone that receives inputs only from the contralateral eye, and a small binocular zone (BZ) that receives inputs from both eyes[10,11] (**Fig. 1a**). Within this BZ, the effects of monocular deprivation (MD) can be detected physiologically after eye closure. Microelectrode recordings have shown that 3–5 d MD during a defined critical period between P25 and P35 shifts OD towards the open eye[12,13], consistent with previous observations in higher mammals. However, clear anatomical rearrangement of thalamocortical projections cannot be detected in mice without long periods of MD (40 d)[14]. This contrasts with the rapid rearrangements in OD columns that occur within 4–7 d after MD in cats and monkeys[15]. Although there are similarities between mice and higher mammals in visual plasticity, there are also substantial differences[14].

Our understanding of visual plasticity in mouse has been based primarily on single-unit extracellular recordings from cortical neurons, in which the relative balance of inputs representing each eye is assessed within the BZ[12,13]. This method requires visually driven inputs to be strong enough for postsynaptic spiking. However, visually evoked potential (VEP) recordings, thought to reflect primarily excitatory synaptic inputs, have recently revealed surprising OD plasticity in the BZ of adult mice[9]. Moreover, the less-represented ipsilateral eye inputs, which could be more susceptible to visual deprivation, have not

been studied extensively. Here, a functional technique based on *in situ* hybridization for the immediate early gene *Arc*[16] is used to investigate pathways representing the ipsilateral eye in developing and adult mouse visual cortex and after visual deprivation. We find multiple periods of susceptibility to visual deprivation in mouse visual cortex.

## RESULTS

### *Arc* maps functional connections driven by each eye in VC

To determine the spatial pattern of functional inputs representing each eye across visual cortex (VC), we used immediate early gene activation, which leaves a lasting trace in tissue sections[17–19]. *Arc* was selected because it is highly and rapidly upregulated after visual stimulation. The BZ was clearly evident after 30 min of monocular visual stimulation as a small patch of *Arc* expression at the border between V1 and V2 ipsilateral to the stimulated eye; *Arc* expression was present throughout VC contralateral to the stimulated eye (**Fig. 1b**; briefer periods did not induce robust levels of *Arc* mRNA by the ipsilateral eye; data not shown). The expected broader representation of the BZ at more caudal visual cortical locations[14,20,21,22] was also present (**Fig. 1c**). Induction of *Arc* depended on visual stimulation, as there was no induction in binocularly enucleated mice (**Fig. 1d**).

*Arc* mRNA hybridization signal after induction was heavy in two bands of cortex corresponding to layers 2–4 (ref. 23) and layer 6, and it was lowest in layer 5 (ref. 24; **Fig. 1e**). Double *in situ* hybridization showed that induction was restricted to CaMKIIα-expressing neurons, not GAD67-expressing neurons (**Fig. 1f**), indicating that *Arc* mRNA could be induced in a large cohort of excitatory neurons[25].

*Arc* induction was compared to the anatomical pattern of geniculo-cortical projections (**Fig. 1g**). As expected[14,26,27], transneuronal label was widely distributed throughout layer 4 of VC contralateral to the injected eye and was restricted to a distinct patch ipsilateral to the

---

[1]Department of Neurobiology, Harvard Medical School, 220 Longwood Avenue, Boston, Massachusetts 02115, USA. [2]Current address: Department of Biophysics, Kyoto University Graduate School of Science, Kitashirakawa-Oiwake-cho, Sakyo-ku, Kyoto 606-8502, Japan. [3]These authors contributed equally to this work. Correspondence should be addressed to C.J.S. (carla_shatz@hms.harvard.edu).

**Figure 1** The pattern of *Arc* induction reliably reflects the pathways activated by visual stimulation. (**a**) Illustration of mouse visual system. Binocular zone (arrowhead) is located at the border between primary (V1) and secondary (V2) visual cortex. (**b**) *In situ* hybridization showing pattern of *Arc* mRNA induction in P34 mouse brain after monocular visual stimulation. Arrowhead: restricted distribution of *Arc* mRNA in binocular zone of visual cortex ipsilateral to stimulated eye. Cx, cortex. Hc, hippocampus. Scale bars (**b,c,d**), 500 µm. (**c**) Representation of ipsilateral eye in rostral, middle and caudal regions of visual cortex as assessed by *Arc* induction. Arrowheads indicate BZ. (**d**) Lack of *Arc* mRNA induction after binocular enucleation. (**e**) Laminar analysis of *Arc* induction (left). Cresyl violet staining (CV) and *in situ* hybridization with layer-specific probes (RORβ, layer 4 specific[23]; ER81, layer 5 specific[24]) were performed on adjacent sections. Scale bar, 200 µm. (**f**) Visual stimulation upregulates *Arc* expression specifically in excitatory neurons: double *in situ* hybridization with ^{35}S-labeled *Arc* probe and DIG-labeled cell type–specific markers (CaMKIIα, excitatory; GAD67, inhibitory). *Arc* expression coincides with most (87 of 91) CaMKIIα-expressing neurons (arrowheads), and never (0 of 82) with GAD67 expression (small arrows, *Arc* positive and GAD67 negative; large arrows, *Arc* negative and GAD67 positive). In this bright-field autoradiograph, silver grains appear black. Scale bar, 25 µm.



(**g**) Pattern of thalamocortical projection visualized by transneuronal transport of [^{3}H]proline injected into one eye (^{3}H-AA). Note band of strong signal in cortex contralateral to injected eye (contra), and small patch (arrowhead) in cortex ipsilateral to injected eye (ipsi). Scale bar, 500 µm. (**h**) Coexpression of *Arc* and BDNF mRNAs in OD columns in cat VC. Activity in one eye was blocked for 48 h by a single intraocular injection of TTX at P43. Adjacent sections were hybridized with either *Arc* or BDNF riboprobe; *in situ* hybridization shown in dark-field optics. Merged image: green, *Arc* mRNA; red, BDNF mRNA. (**i**) Complementary pattern of OD column labeling and *Arc* induction in adult cat visual cortex. Geniculocortical axons in layer 4 (arrowheads) were labeled by transneuronal transport of [^{3}H]proline (see Methods) and adjacent sections hybridized for *Arc* mRNA (arrows). Merged image: green, *Arc* mRNA; red, transneuronally transported label. Scale bar (**h,i**), 500 µm.
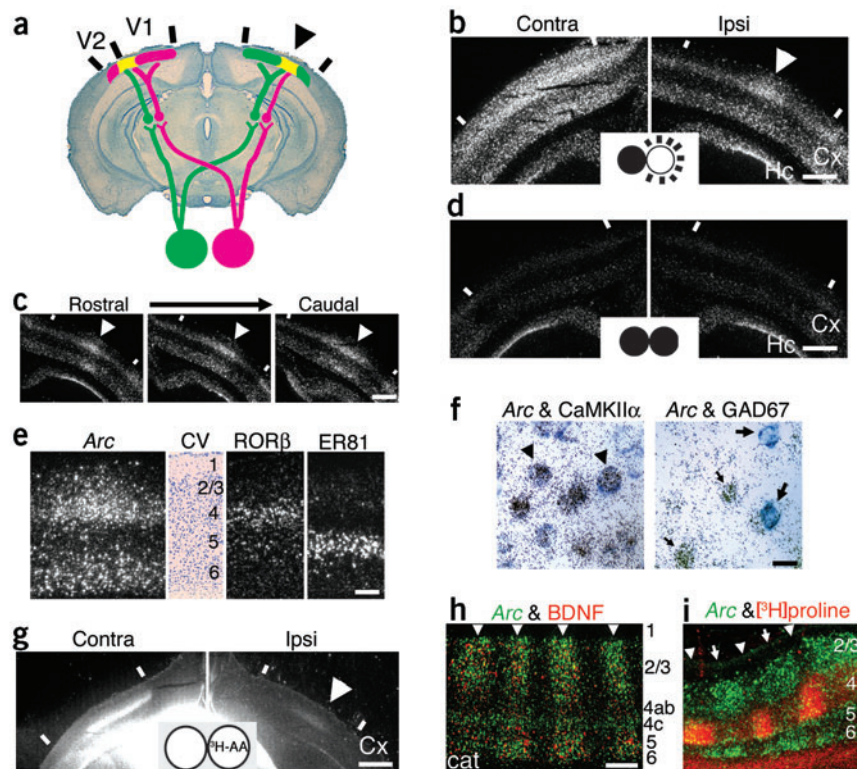
injected eye (the BZ). This pattern was similar to *Arc* induction patterns (**Fig. 1b,1g**), though slightly more restricted horizontally, since Arc shows ipsilateral eye activation of cortical neurons, whereas the transneuronal transport method exclusively reflects the pattern of presynaptic geniculocortical axons in layer 4.

The spatial pattern of *Arc* induction also reflects accurately known OD distributions in the cat, where stimulation of one eye activates vertical columns throughout VC[3]. Monocular TTX injection rapidly downregulates BDNF mRNA within OD columns linked to the inactive eye[28], with high expression maintained within active eye columns (**Fig. 1h**). An almost identical columnar pattern was present after *Arc* induction (**Fig. 1h**). To confirm that vertical columns of *Arc* mRNA belonged to the stimulated eye, transneuronal tracer was injected into one eye[26,29], and the other eye was stimulated visually for 30 min, resulting in interdigitating columns of label representing inputs from either eye (**Fig. 1i**). The low *Arc* signal in OD columns belonging to the unstimulated eye also suggested that the visual stimulation protocol did not saturate or elevate background nonspecifically. Collectively, *Arc* induction provides an excellent signal-to-noise ratio, and its spatial patterns resemble known functional and anatomical distributions of inputs representing the two eyes to mouse and cat VC[9,20–22].

### Developmental changes in the ipsilateral representation

In the formation of OD columns in higher mammals, geniculocortical connections representing the two eyes are initially more widespread and then are remodelled[26,30,31]. Transneuronal transport of WGA-HRP or [^{3}H]proline has been used in mouse to monitor developmental changes in the ipsilateral eye representation and formation of the BZ[32]. However, these anatomical methods are unreliable at early ages. Therefore, we used *Arc* induction as a different, functional (rather than anatomical) means for assessing ipsilateral eye input at early ages.

At P14, *Arc* induction in response to monocular stimulation was no higher than background expression (data not shown). By P17, *Arc* mRNA was induced across the entire mediolateral VC contralateral to the stimulated eye (**Fig. 2a**), as expected given the extensive representation of the contralateral eye. Notably, a similar, widespread pattern of *Arc* induction was also present ipsilateral to the stimulated eye. This pattern at P17 did not reflect high basal levels of *Arc* mRNA in immature cortex, as no *Arc* signal could be detected in the absence of visual stimulation (**Fig. 2b**). Thus, *Arc* signal at P17 reflects the functional representation of the stimulated eye, suggesting that the ipsilateral eye's influence on cortical neurons is not restricted to the BZ at this early age but instead may be broadly distributed across VC. An adult-like restriction of the ipsilateral eye's representation emerged during the next week (**Fig. 2a**), so that by P25, the *Arc* induction pattern narrowed into the BZ; this restricted pattern persisted into adulthood. In contrast, the contralateral eye representation was distributed across the entire VC at all ages.

Anatomically, at P17, retinal inputs have already segregated into LGN layers for more than 1 week[33–35]. It is possible, however, that ipsilateral retinal inputs are still able functionally to activate neurons throughout

**Figure 2** Developmental restriction of ipsilateral eye representation in visual cortex between P17 and P25. (**a**) *Arc* mRNA *in situ* hybridization after 30-min monocular visual stimulation at P17 (top), P22 (middle) or P25 (bottom) in cortex contralateral (left) or ipsilateral (right) to the stimulated eye. Scale bar, 500 μm. (**b**) No *Arc* induction was seen in the absence of visual stimulation at P17. (**c**) Pattern of *c-fos* induction in LGN after visual stimulation of right eye at P17. Top: diagram of retinogeniculate projection. Retinal axons from contralateral eye occupy most of the LGN, with a small zone receiving input from the ipsilateral eye. Bottom: *in situ* hybridization showing restricted pattern of *c-fos* mRNA induction in LGN ipsilateral to the stimulated (right) eye. Arrows indicate ipsilateral eye projection zones. dLGN is outlined. Scale bar, 300 μm. (**d**) Ratio of *Arc* mRNA signal intensity in monocular zone (MZ) relative to binocular zone (BZ). Error bars, s.d. 8–12 sections each were scanned from three mice at each age. Ipsilateral eye ratio (filled squares) decreases until P25, whereas contralateral eye ratio (open squares) does not. (**e**) Densitometric line scans of *Arc* mRNA signal in layer 4 across the entire mediolateral extent of V1 and V2 from a representative *in situ* hybridization section after stimulation of ipsilateral eye at P17, P25 or P96. The region of ipsilateral eye representation, determined by an automated program, is shown in each image. Raw trace (thin line) and low-pass filtered trace (solid line) are indicated. Horizontal line marks threshold; vertical lines mark borders of *Arc* induction above threshold in V1 and V2; scan peak is located in center of BZ (see Methods). (**f**) Averaged line scans at multiple ages (P17, P22, P25, P56) aligned to the background value in V2. The average scans show a similar pattern of induction as individual scans above. The signal increases from minima in V1 and V2 to a maximum. Vertical lines indicate the borders of Arc signal induction above background in V1 and V2. Horizontal lines indicate width of Arc induction at the different ages and show that width of the BZ decreases with age. (**g**) Top: width of zone representing ipsilateral eye in layer 4 declines until P25, as assessed in densitometric scans of autoradiographs of *Arc* mRNA *in situ* hybridizations. Bottom: *Arc* induction by ipsilateral eye, as assessed by densitometric scans of mRNA signal intensity in layer 4, increases between P17 and P25. At each age, 11–18 sections from three mice were scanned.
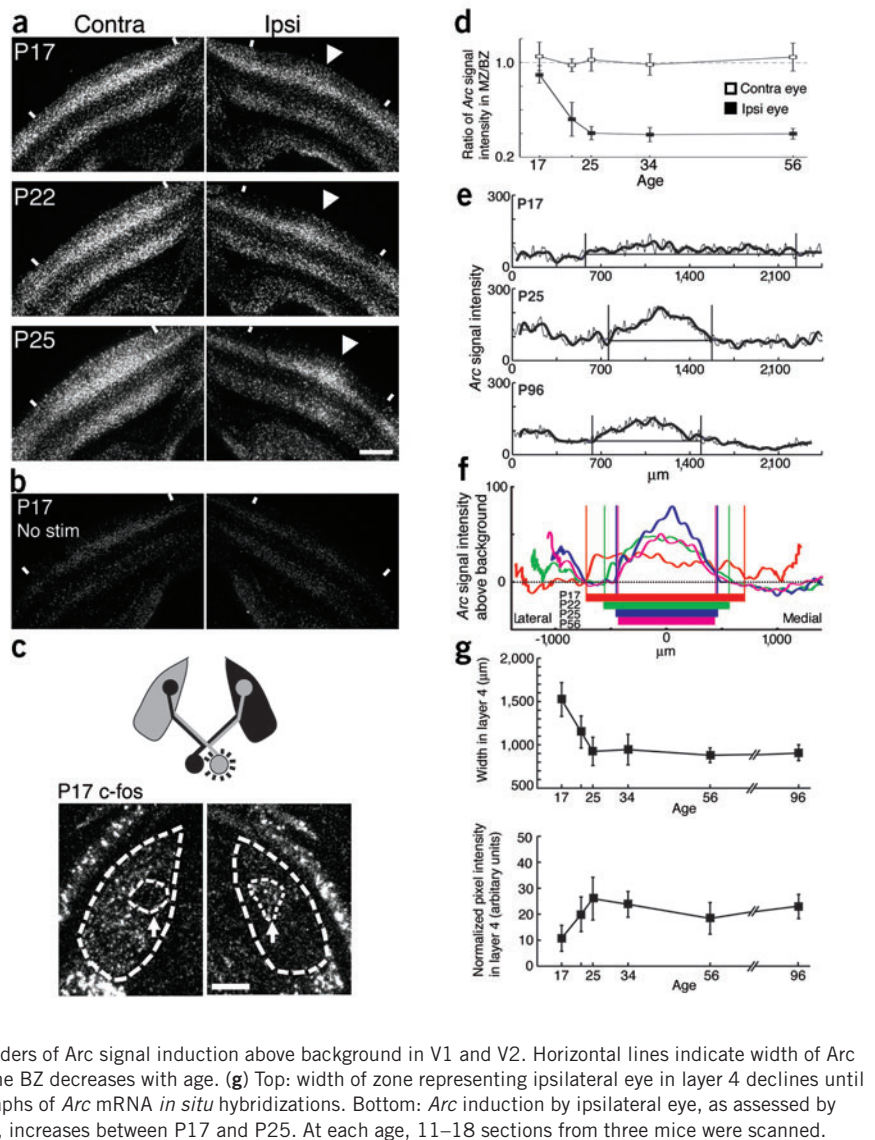


the LGN. Thus, we carried out *in situ* hybridization for the immediate early gene *c-fos* (also known as *Fos*) in adjacent LGN sections (*Arc* is not expressed in the thalamus at any age). Within the dorsal LGN ipsilateral to the stimulated eye, *c-fos* induction was confined to a small zone; contralateral to the stimulated eye, it was induced in a large region of the LGN with a gap corresponding to the projection from the ipsilateral eye (**Fig. 2c**). This pattern mirrors the adult patterns of segregated retinal axons from the two eyes. Thus, the widespread pattern of *Arc* induction in VC is not a consequence of unrestricted activation of LGN neurons.

These observations were validated quantitatively using two methods. First, the ratio of *Arc* signal intensities in monocular versus binocular zones was compared at each age (**Fig. 2d**; Methods). The ratio did not change with age in cortex contralateral to the stimulated eye, but ipsilaterally, the ratio decreased between P17 and P25, validating the observed decline in *Arc* mRNA *in situ* hybridization signal outside the BZ at progressively older ages. Second, to eliminate any bias introduced by having to decide the location of monocular or binocular zones at early ages, densitometric scans were made (**Fig. 2e**; Methods) of autoradiographs of *Arc* mRNA *in situ* hybridizations along layer 4 across all of VC (including V1, V2 and the intervening BZ; **Fig. 1a**). *Arc* signal induced

by the ipsilateral eye increases from a minimum in V2 to a maximum and then decreases again, a pattern evident in averaged scans at all ages examined (**Fig. 2f**). The width of the zone activated by the ipsilateral eye declines from P17 to P25 and remains stable thereafter (**Fig. 2f,g**). The intensity of the hybridization signal (**Fig. 2f,g**) also showed a progressive increase in the strength of *Arc* induction between P17 and P34. Collectively, these observations suggest that between P17 and P34 there is a period of functional sculpting and strengthening of the ipsilateral eye representation to form the BZ within VC.

To further support this suggestion, retrograde tracer was injected into the VC to assess thalamocortical projections at P19 anatomically. In adult, projections from LGN neurons representing the ipsilateral eye are restricted to the BZ. If the widespread *Arc* induction at P19 reflects direct projections from LGN neurons, the extent of retrograde labeling in the LGN after tracer injection into the BZ should be greater than that seen at older ages. Indeed, red retrobeads injected into the lateral part of VC (**Fig. 1a**: BZ) labeled about two times the area of LGN at P19 than at P37 (**Supplementary Fig. 1** and **Supplementary Methods** online). This implies that the widespread pattern of *Arc* induction seen at P19 reflects, at least in part, thalamocortical projections that are also
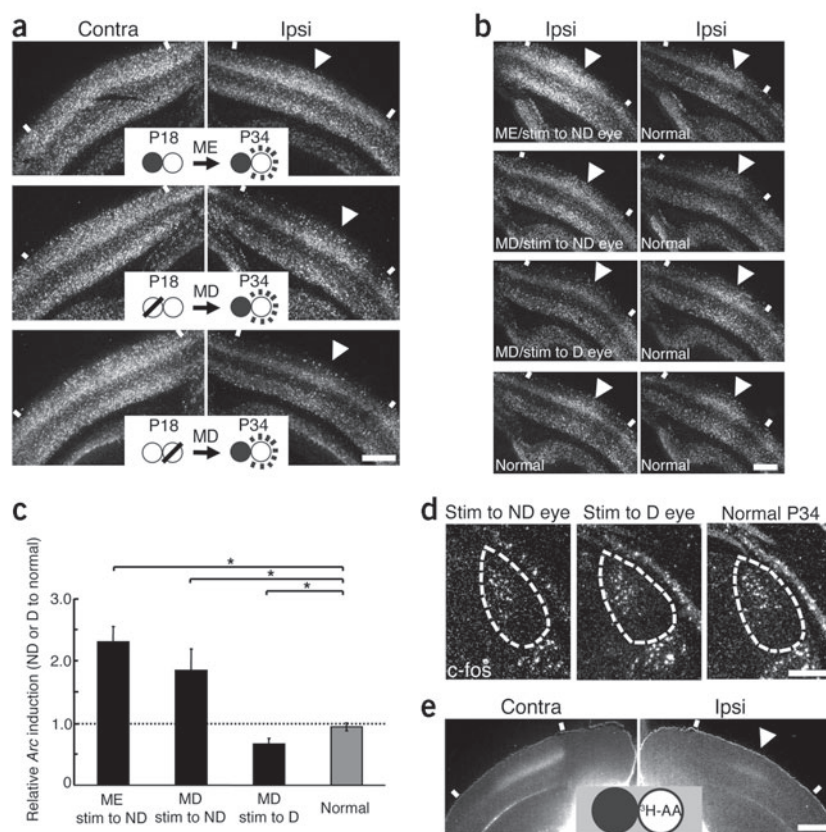
**Figure 3** *Arc* induction shows OD plasticity induced by ME or MD during the known 'critical period'. (**a**) ME (top) or MD (middle and bottom; diagonal bar indicates deprived eye) was performed at P18, and *Arc* induction in VC was assessed by stimulating either the nondeprived eye (top, middle) or deprived eye (bottom) at P34 (stimulated eye is shown in white). Compared with that in normally reared mice (**Fig. 1b**), the spatial extent of *Arc* induction in VC ipsilateral to the nondeprived eye was broader (top and middle); induction in VC ipsilateral to the deprived eye was more restricted (bottom). Scale bars in **a** and **b**, 500 µm. (**b**) Pairwise comparison of *Arc* induction. Sections from ME or MD mice were paired with those from normal mice on the same glass slide and processed in parallel. Each pair shows *Arc* induction in the binocular zone after 30 min visual stimulation of the ipsilateral eye at P34. Top pair: nondeprived (ND) eye was stimulated after ME at P18. Second pair: MD was performed at P18 and ND eye was stimulated at P34. Third pair: MD at P18 followed by stimulation of the deprived (D) eye at P34. Bottom pair: sections from different normal mice show reproducibility of *Arc* induction. (**c**) Relative *Arc* induction calculated from paired images such as those in **b**: ME stimulus to ND, $2.30 \pm 0.25$, $P = 0.017$; MD stimulus to ND, $1.85 \pm 0.34$, $P = 0.017$; MD stimulus to D, $0.66 \pm 0.10$, $P = 0.014$; $n = 7$–8 pairs of sections in four mice for each treatment. Error bars, s.d. *$P < 0.05$, Mann-Whitney test. (**d**) *c-fos* induction in the LGN (outlined) ipsilateral to the stimulated eye after various treatments. Scale bar, 300 µm. (**e**) A representative autoradiograph of VC from a mouse that received ME at P18, [³H]proline injection into the ND eye at P35 and was examined at P40. The pattern of thalamocortical projection does not seem altered by ME at P18 (compare with **Fig. 1g**). Scale bar, 500 µm. Arrowheads in **a**,**b**,**e** indicate location of binocular zone.

more broadly distributed than at later ages. However, it is possible that horizontal connections within cortex also contribute to the widespread *Arc* induction at the youngest ages.

### *Arc* induction detects OD shifts during a critical period

In rodents, as in higher mammals, monocular deprivation (MD) during a critical period causes functional shifts in connectivity in favor of the nondeprived eye, as shown by microelectrode and VEP recordings[9,12,13,36]. To assess whether *Arc* induction can detect such functional plasticity, we first examined mice after long periods (2 weeks) of deprivation. One eye was enucleated (ME) or sutured closed (MD) at P18, and mice were reared in a normal environment until P33; mice were then placed in the dark at P33, and *Arc* induction was examined 24 h

later by visually stimulating either the nondeprived eye (NDE), or the deprived eye (DE) in MD mice, for 30 min. We began deprivation at P18 based on observations (discussed above) of an early period during which the ipsilateral eye input is widespread. Deprivation was ended at P34 because the critical period for the effects of brief MD concludes at about this time[9,12,13]. The intensity of *Arc* induction by the ipsilateral NDE was increased after either ME or MD in these mice as compared with unmanipulated mice at P34 (**Fig. 3a**, top and middle, versus **Fig. 3b**, normal), consistent with the strengthening of ipsilateral NDE inputs shown previously by VEP or intrinsic signal optical recordings[9,14].

*Arc* induction also extends our understanding of the functional organization of the DE and NDE after deprivation (**Figs. 3** and **4**). First, after MD, the ipsilateral, DE representation in the BZ was weaker than normal, as assessed by the intensity of *Arc* mRNA signal, and was restricted to a very narrow region at the V1-V2 border (**Fig. 3a**, bottom). Many previous studies have shown a weakening of the DE input to contralateral cortex during the critical period[9,12–14]. However, weakening of the deprived ipsilateral eye, as observed here with *Arc* induction, has been reported only with single-unit[13] or optical imaging methods[14]. Second, we found, unexpectedly, that the spatial extent of *Arc* induction by the ipsilateral NDE was much broader than normal, resembling the distribution seen at earlier developmental ages (compare **Fig. 3a,b** with **Fig. 2** at P17). In contrast, signal intensity and spatial distribution of *Arc* induction contralateral to the NDE did not seem to change.

To validate these impressions, cortical sections from ME or MD mice were mounted on the same glass slide with those from normally reared mice and processed simultaneously for direct, pairwise comparison (**Figs. 3b,c**). After ME or MD from P18 to P34, *Arc* induction by stimulation of the ipsilateral NDE was 200% of normal (**Fig. 3c**). In contrast, *Arc* induction by the DE decreased to about 50% of normal (**Fig. 3c**).

The changes in strength and spatial extent of the ipsilateral eye representation in cortex are unlikely to be due to deprivation-induced changes in the LGN, as *c-fos* induction was indistinguishable in the LGN from deprived and normally reared mice, whether the stimulated ipsilateral eye was deprived or nondeprived (**Fig. 3d**). The expanded spatial distribution of *Arc* induction by the ipsilateral NDE might also reflect a widespread distribution of LGN projections to layer 4. Yet the geniculocortical projection pattern from the NDE to both hemispheres seems indistinguishable from normal (**Figs. 1g** and **3e**), consistent with previous studies of mice that underwent MD for a similar duration[14]. Thus, the changes in *Arc* induction intensity and spatial extent are likely to reflect changes at or beyond thalamocortical connections.

**Figure 4** Visual experience alters initial formation and subsequent maintenance of ipsilateral eye representation within visual cortex. (**a**) ME or MD was performed at P17, and *Arc* induction after 30-min stimulation of ipsilateral eye in VC was assessed at P25. (**b**) After developmental sculpting was completed around P25 (see **Fig. 2**), 1 week of ME or MD could still modify the representation of the ipsilateral eye as assessed by *Arc* induction. Scale bar, 500 μm. (**c**) Representative examples of densitometric scans of *Arc* mRNA signal in layer 4 across the entire mediolateral extent of V1 and V2 after stimulation of ipsilateral eye under different rearing conditions. Top: ME at P25 and ND eye stimulated for 30 min at P34. Middle: MD at P25 and D eye stimulated. Bottom: normally reared until *Arc* induction experiment at P34. The area of ipsilateral eye representation, determined by an automated program, is shown in each image. Arrows indicate periodic fluctuation seen in MD animal (see text). Raw trace (thin line) and low-pass filtered trace (solid line) are shown (see Methods for more details). (**d**) Width of the area of ipsilateral eye representation in layer 4 measured from densitometric scans of *Arc in situ* signal. Solid line, normal development (from **Fig. 2g**); open squares, ND eye; filled squares, D eye. At each age, deprivation was performed 7–11 d before *Arc* induction experiment. For each time point, 11–18 sections from three animals were scanned. The ipsilateral, nondeprived eye was consistently greater than normal at every eye including at P96 ($P < 0.001$ at all ages). (**e**) Pattern of *in situ* hybridization for *Arc* mRNA (green) and transneuronal labeling of LGN axons in layer 4 (red) of cat visual cortex at P42. Left: columnar organization of *Arc* induction at P42 after visual stimulation of one eye in an unmanipulated animal; the other eye was injected with [3H]proline for transneuronal labeling of LGN projections (red). Middle: MD from P32–42 resulted in expanded *Arc* induction by the NDE and narrower LGN projections representing the DE in layer 4. Right: narrow columns of *Arc* induction by the DE; LGN projections representing the NDE were expanded. Layer 4 borders are indicated to the right of panels. Scale bar, 1 mm.
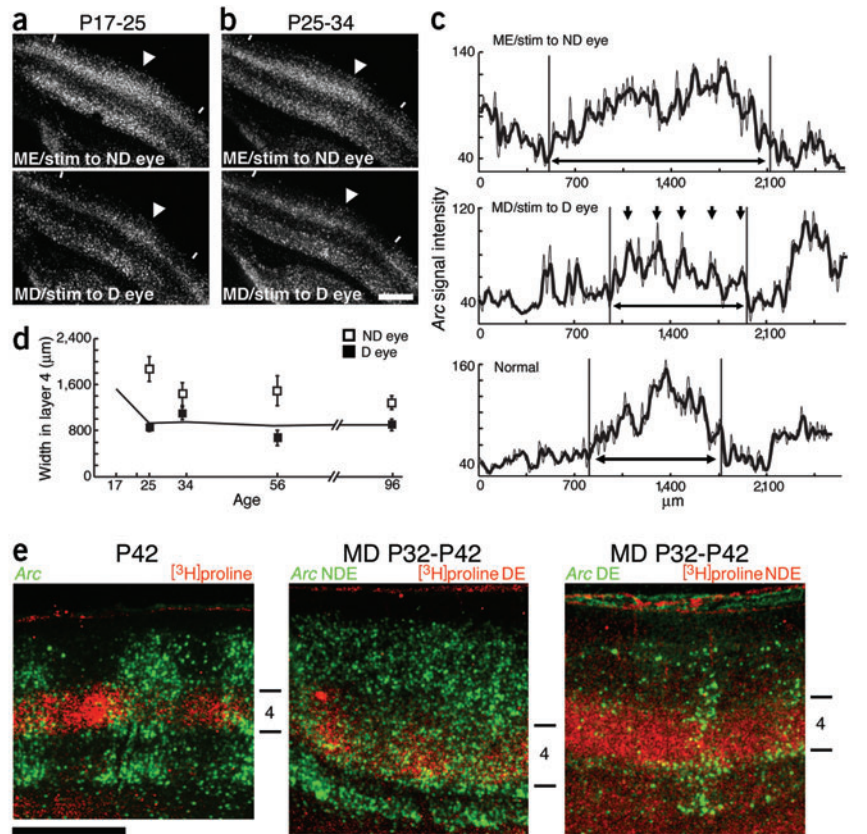


Previous single-unit recording studies have reported a weakening of the DE inputs to contralateral cortex within the mouse BZ during but not after the critical period[12,13], but *in situ* hybridizations for *Arc* mRNA did not show a similar decrease in *Arc* induction by the contralateral DE (compare **Fig. 3a**, bottom left, with **Fig. 1b**). To clarify this discrepancy between methods, we quantified *Arc* mRNA in cortex after MD from P18–34 by real-time PCR (Methods). In ipsilateral cortex after stimulation of the DE, real-time PCR detected the expected decrease in *Arc* mRNA (P34: 67% of unmanipulated; $n = 6$ pairs of mice; $P < 0.05$). However, in cortex contralateral to the DE, there was no significant decrease in *Arc* mRNA relative to unmanipulated controls ($P > 0.2$). Thus, two independent methods (PCR and *in situ* hybridization) show that there is no detectable change in *Arc* mRNA contralateral to the DE. The difference between *Arc in situ* hybridization and single-unit recordings may be due to the fact that the single-unit recordings give a local ratio of the balance between the DE and NDE at one location (such as in the BZ), whereas the *Arc* method is averaged across both MZ and BZ. In addition, visual stimulation used in this study was optimized to assess the pattern of *Arc* induction by the ipsilateral eye; shorter visual exposures might show a weakening of *Arc* induction by the contralateral DE. These further considerations imply that *Arc* induction ipsilateral to the stimulated eye, whether the eye is deprived or nondeprived, provides a reliable assessment of the functional state of ocular inputs to mouse visual cortex.

## OD formation and maintenance require visual experience

As shown above, the representation of the ipsilateral eye in cortex is widespread at P17 and then restricted by P25 during normal development. Visual deprivation could alter normal development from P17–P25, change the representation of the ipsilateral eye at later times (P25–34) or affect both periods. To examine these possibilities, the deprivation period was subdivided into two separate 1-week periods. After MD from P17–25, *Arc* induction by the ipsilateral NDE extended well beyond the normal BZ (compare **Fig. 4a** and **2a**). Normally, *Arc* induction at P17 is widespread, so this result suggests that MD at these early ages prevents the normal developmental restriction of ipsilateral inputs representing the NDE into the BZ. Furthermore, *Arc* induction ipsilateral to the DE was lower than normal, suggesting that inputs from the DE have weakened.

Because the normal adult-like restriction of the ipsilateral eye to the BZ occurs by P25 (**Fig. 2**), we examined the effect of later deprivation (**Fig. 4b**). ME or MD from P25–P34 causes widespread induction of *Arc* across VC after stimulation of the ipsilateral NDE; this is a genuine expansion of the normally restricted pattern at P25 (compare **Fig. 2**). *Arc* induction by the ipsilateral DE after MD from P25–34 was fainter than normal at P25 (**Fig. 4b**, bottom), suggesting a loss of connectivity.

Quantitative analyses of *Arc* induction in layer 4 supported these observations (**Figs. 4c,d**). Densitometric scans of *Arc in situ* hybridization signals showed that the ipsilateral NDE occupied a broader-than-
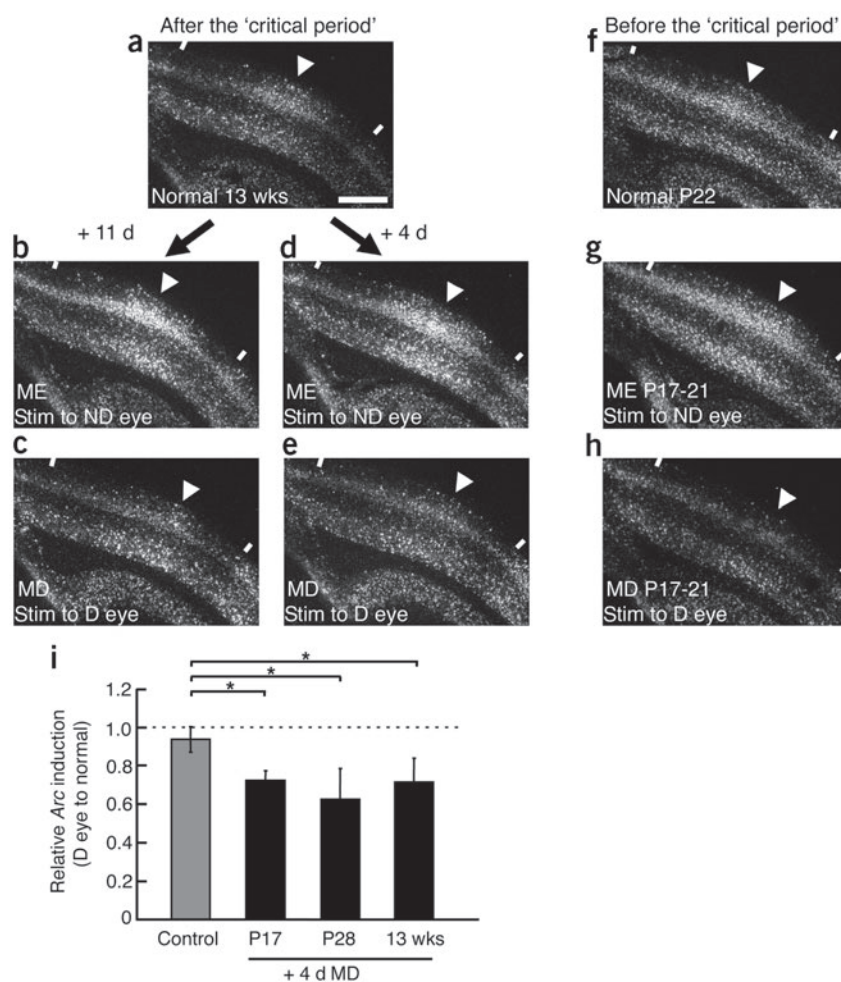
**Figure 5** *Arc* induction shows OD plasticity earlier and beyond the known 'critical period'. (**a**) Normal pattern of *Arc* induction at 13 weeks. (**b**,**c**) Effect of long-term (11-d) ME or MD on *Arc* induction. After ME, extent of *Arc* induction after 30-min stimulation of the ipsilateral NDE is increased and expanded (**b**), whereas *Arc* induction is decreased after stimulation of the ipsilateral, DE after MD (**c**). Scale bar, 500 μm. (**d**,**e**) Short-term (4-d) manipulations cause similar effects as long-term. (**f**) Normal pattern of *Arc* induction at P22. Area of *Arc* induction is not yet restricted to a binocular zone, but there is a clear peak of *Arc* signal (arrowhead). (**g**,**h**) Changes in extent of *Arc* induction similar to those at older ages are evident after 4-d ME or MD begun at P17. (**i**) Comparison of the effects of 4-d MD on *Arc* induction before, during or long after the 'critical period'. MD done at P17, P28, or 13 weeks, and *Arc* induction assessed 4 d later. Coronal sections from MD animals were mounted on same glass slide with those from age-matched controls and processed together for *in situ* hybridization. In each pair, the ratio of the intensity of *Arc* induction by DE to normal was calculated (see Methods). P17, 0.72 ± 0.05, $P = 0.014$; P28, 0.63 ± 0.16, $P = 0.011$; 13 weeks, 0.72 ± 0.12, $P = 0.041$; $n = 8$–10 pairs of sections in four animals for each age. Error bars: s.d. *$P < 0.05$, Mann-Whitney test.

NDE expanded in all layers of cortex, whereas columns driven by the DE were narrower than normal (**Fig. 4e**). Thus, *Arc* induction patterns in the cat after MD reported expected changes in OD column width for both the deprived and the nondeprived eyes. Although the way in which the functional representation of the ipsilateral DE changes after MD may differ somewhat between cat and mouse, in both cases *Arc* induction indicated a decrease.

## OD plasticity in adult VC and before the critical period

In mouse, single-unit microelectrode recordings have defined P25–P35 as a 'critical period' for OD plasticity after 3–5 d of MD; OD shifts have not been observed by this method after similar MD at older ages[12,13]. However, VEP recordings detected OD shifts towards the NDE after MD in adults[9]. To clarify these observations, we examined whether longer periods of MD or ME resulted in detectable OD shifts assessed by *Arc* induction. Eleven days of MD begun at P44 (data not shown) or in adults at 13 weeks of age (**Fig. 5**) resulted in shifts in the representation of the ipsilateral eye within VC (**Fig. 5a**). *Arc* induction after stimulation of the ipsilateral NDE appeared more intense and extended beyond the limits of the normal BZ (**Fig. 5b**). In contrast, *Arc* induction after stimulation of the ipsilateral DE was fainter than normal (**Fig. 5c**) (P56: 63.5% of normal, $P = 0.005$; 13 weeks: 72.3% of normal, $P = 0.007$). Densitometric scanning of layer 4 confirmed these observations quantitatively (**Fig. 4d**). In contrast, similar scans confined to layer 6 did not show significant changes in the width of *Arc* induction by the ipsilateral NDE at either P56 or 13 weeks, whereas changes in layer 6 were detected at P34 (155% of normal, $P < 0.005$). Together, these results suggest that a robust form of OD plasticity exists in the superficial (but not deep) cortical layers at older ages in mouse VC, at least with longer periods of monocular deprivation.

In view of the plasticity revealed by *Arc* induction at older ages (**Fig. 4d**), we sought to validate the effects of brief 3–5 d periods of

normal territory across VC (**Fig. 4c**, top and bottom). ME from P17–25 also results in a wider ipsilateral NDE representation than normal in P17 (**Fig. 4d**). In contrast, we did not detect a change in the overall spatial extent of the ipsilateral DE representation after MD. However, there was decreased *Arc* signal intensity and a marked periodic fluctuation of the *in situ* hybridization signal for the ipsilateral DE (**Fig. 4c**, middle). Consequently, overall *Arc* induction as measured by normalized pixel intensity was lower: 56.8% of unmanipulated control ($P = 0.009$). Similar results were seen with visual deprivation from P25–34 (53.4% of unmanipulated control, $P < 0.001$). These observations suggest that after 1 week of MD during the critical period, the ipsilateral representation of the DE within cortex weakens considerably. Thus, in mouse, deprivation-induced OD shifts can be detected in the BZ by *Arc* induction during the known critical period (P25–P34), consistent with results from single unit recordings[13]. However, we now find that not only the relative physiological balance of inputs representing the DE and NDE, but also the spatial extent of the input from the ipsilateral eye, depends on visual experience during this period.

In mouse, MD during the critical period expands and strengthens *Arc* induction ipsilateral to the NDE, and it weakens but does not decrease the spatial extent of *Arc* induction ipsilateral to the DE. However, in cat or monkey after MD, OD columns representing the deprived eye shrink anatomically and physiologically[3,29,30]. To examine whether *Arc* induction could detect this species difference, cats received MD from P32 to P42 (the height of the critical period). Then *Arc* induction by NDE ($n = 2$ animals) or the DE ($n = 2$ animals) was assessed. *Arc in situ* hybridization showed that OD columns driven by stimulation of the

MD or ME on OD during the known critical period (**Fig. 5**). As with microelectrode recordings, *Arc* induction also showed that 4 d of MD between P28 and P32 weakens ipsilateral inputs driven by the DE within the binocular zone of cortex (**Fig. 5i**). As with the longer-duration deprivation experiments (**Fig. 4**), 4 d of MD also caused the pattern of *Arc* induction within the BZ to become patchy, consistent with a report[13] that brief MD during the critical period in mouse VC weakens ipsilateral DE within the BZ. In addition, *Arc* induction showed shrinkage of the spatial representation of the DE within VC after very brief periods of MD during the critical period (**Fig. 5i**). Both weakening and shrinkage could account for the shift in OD towards the NDE during the critical period seen with microelectrode recordings.

Notably, in mice at 13 weeks, even a 4-d deprivation resulted in clear OD plasticity: *Arc* hybridization signal after stimulation of the ipsilateral DE was spatially more restricted (**Fig. 5e**) and weaker (**Fig. 5i**). Real-time PCR also detected this decrease in *Arc* induction by the DE in ipsilateral cortex (30% of unmanipulated; $P < 0.05$, $n = 5$ pairs of mice) after 4 d of MD in adults. No decrease was seen in *Arc* induction by the DE in contralateral cortex ($P > 0.2$), consistent with the *in situ* hybridization observations. In addition, *Arc* induction increased in intensity and expanded spatially after stimulation of the ipsilateral NDE (**Figs. 5a,d**). These changes are clearest in the superficial cortical layers (2–4) and not obvious in layer 6. OD plasticity has been reported recently in the adult mouse VC using VEP recordings, but was thought to be confined to the BZ and to represent strengthening of the ipsilateral NDE exclusively[9]. Expanded representation of the ipsilateral NDE into the MZ, normally driven by the contralateral eye, after as little as 4 d of MD is an unexpected outcome of using *Arc* induction to monitor OD shifts.

We also examined whether 4 d of MD at earlier ages, before the critical period, result in OD shifts. *Arc* induction by the ipsilateral NDE after MD from P17 to P21 was more intense and widespread in most of VC (**Figs. 5f,g**); *Arc* induction by the ipsilateral DE was weaker (**Fig. 5h,i**). This result implies that certain forms of OD plasticity have gone undetected in mouse VC using microelectrode or VEP recordings.

## DISCUSSION

Here we have used *Arc* induction to monitor the functional representation of eye input in the mouse VC during normal development and also after manipulations that create imbalances in inputs from the two eyes, such as MD or ME. Our observations using this method not only confirm several prior key observations on OD plasticity but also include unexpected findings suggesting that mouse VC is capable of plastic changes earlier and much later than previously described. In addition, because *Arc* induction permits a direct functional assessment of ipsilateral eye input, we discovered a previously unknown malleability in the spatial extent of the ipsilateral eye representation within VC. MD or ME, both during and after the known critical period (P25–34; ref. 12), cause an expansion of the ipsilateral NDE representation far beyond the normal confines of the BZ, which has not been reported in any species to date. This implies that mouse VC, while presenting important opportunities for genetic manipulation, may not be identical to the VC of highly binocular mammals such as cat or monkey with regard to critical period mechanisms.

### *Arc* induction reports OD reliably

The validity of our conclusions rests on how faithfully *Arc* induction mirrors the functional state of inputs from the two eyes within VC. We believe this is the case. First, the original experiments in hippocampus demonstrated a faithful readout of physiological activity in *Arc* mRNA induction patterns[16,19]. Second, *Arc* induction patterns in adult mouse VC after monocular visual stimulation are accurate reflections of the

well-known representations of ipsilateral and contralateral eyes based on microelectrode[13,22], VEP[9,37] or optical[14,20,21] recordings, or anatomical transneuronal tracing methods[14,27]. Furthermore, using the tightly organized system of OD columns in cat VC, we show that stimulation of one eye results in a columnar pattern of *Arc* induction that coincides with known OD column patterns, both with normal rearing and also after MD during the critical period[26,28]. Third, *Arc* induction during the known critical period in mouse VC (P25–P34) reports shifts in OD expected from electrophysiological recording studies[9,12,13]. Fourth, cortical *Arc* induction patterns are unlikely to be an indirect reflection of changes in the LGN because *c-fos* induction in the LGN in the same experiments does not increase the amount of LGN territory activated by the open (stimulated) eye. We stress that this method augments rather than replaces other techniques, and in particular, it adds a way to assess functionally the spatial extent of ipsilateral eye representation in VC.

We report that monocular eye enucleation or brief eye closure (4 d) in the adult (13 weeks) causes a clear OD shift (**Fig. 5i**) as assessed by examining *Arc* induction in layers 2–4. This is unexpected because it indicates that adult mouse VC is capable of more plasticity than previously imagined, but it supports a recent observation based on VEP recordings from the BZ also showing a shift in OD towards the open eye[9]. These two experiments argue for caution in interpreting OD shifts in adult mouse VC[38].

The *Arc* induction method also provides new information about the spatial extent and laminar pattern of plasticity in each experimental condition. We find OD plasticity in layers 2–4 of adult mouse VC, but *Arc* induction within layer 6 after MD in adult mouse was not substantially different. Because previous electrophysiological recordings[9] have been made only from the upper cortical layers, this essential laminar difference was overlooked. Our results suggest that in adulthood, the deeper cortical layers have more limited plasticity than the upper layers. In this regard, layer 6 of adult mouse VC resembles the cortex of higher mammals[39].

### Ipsilateral eye representation is labile

Notably, the cortical representation of the ipsilateral eye is labile, not only during development but also in adult layers 2–4. Past electrophysiological and optical imaging experiments have focused on the representation of the contralateral eye and have shown that after MD during the critical period, the deprived eye's ability to drive cortical neurons weakens[12–14]. We report a similar weakening of the ipsilateral eye after MD not only during the critical period but also in adulthood. This observation does not agree with a VEP-based assessment of OD plasticity in adult mouse VC[9], which reported strengthening of the NDE, but not weakening of the DE, at this late age. Despite methodological differences in the two techniques, together, the results are consistent with the persistence of OD plasticity in the superficial layers of adult mouse VC.

A new finding is that the representation of the ipsilateral NDE is capable of expanding spatially well beyond the normal limits of the BZ after MD during the critical period; this expansion can occur even in adult mice. Strengthening of NDE inputs has been reported using electrophysiological methods[9], but these studies have focused on cortex within the BZ at the border between V1 and V2, missing the expansion seen in our study. In addition, *Arc* induction permits assessment of the state of OD in unanesthetized animals; this could help explain differences with VEP and microelectrode recordings[40]. The mechanism for the expansion—whether it is driven by changes at thalamocortical synapses in layer 4, via horizontal connections within and beyond layer 4, or both—is not clear, but this expansion of the ipsilateral eye representation detected with *Arc* induction will be useful in characterizing molecular mechanisms of OD plasticity in mutant mice.

### Re-evaluation of the critical period for MD

The *Arc* induction method also permits assessment of the representation of the ipsilateral eye in cortex at times in neonatal development that cannot be studied using VEP, microelectrode recording, optical imaging or even anatomical methods. We have found that at early ages shortly after eye opening (P17), the ipsilateral eye functionally can activate widespread areas of VC. This early widespread, and later restricted, pattern of *Arc* induction by the ipsilateral eye in mouse VC is reminiscent of the remodeling of thalamocortical axons known to occur in the formation of OD columns in the VC of higher mammals[1,4,31].

During this same time period (P14–P21), synaptic scaling in response to monocular deprivation occurs in layer 4 of rodent VC[41,42], and 4-d MD can alter the pattern and intensity of *Arc* induction in VC by the ipsilateral eye, resulting in a spatially expanded representation of the NDE and a weakening in intensity and shrinkage of *Arc* induction by the DE (**Figs. 4** and **5**). Our and others' results[41,42] imply that the critical period for the effects of monocular visual deprivation on cortical physiology begins at or shortly after the time of eye opening: at P14–17 rather than later. Thus, the mouse VC is capable of multiple periods of OD plasticity both during development and, in a more restricted fashion, in adulthood. Although *Arc* induction can show the existence of these periods, the underlying cellular and molecular mechanisms will require additional experiments that examine not only age but also laminar and spatial location within cortex.

### METHODS

All experiments were performed according to the Harvard Medical School Institutional Animal Care and Use Committee Protocol.

**Mouse surgery.** C57Bl/6 mice were used. For monocular enucleation experiments, mice were anesthetized with isofluorane, one eye was removed and pieces of gelfoam inserted in the cavity. Eyelids were trimmed and sutured with 6-0 sterile surgical silk. For monocular deprivation experiments, eyelids were trimmed and sutured. Ophthalmic ointment (Pharmaderm) was used to prevent infection. A drop of Vetbond (3M) was put on sutured eyelids to prevent reopening.

**Arc induction experiments in mouse.** One eye was enucleated 24 h before visual stimulation, and mice were put in total darkness. Mice were returned to a lighted environment for 30 min in the alert condition. After light exposure, mice received an overdose of sodium pentobarbital (1 mg g$^{-1}$ body weight); brains were removed, flash-frozen in M-1 mounting medium (ThermoShandon) and sectioned (coronal plane) at 16 μm for *in situ* hybridization.

**Transneuronal transport of [³H]proline.** To visualize the pattern of geniculocortical projections to layer 4 of cat or mouse VC, 2 mCi (cat) or 150–200 μCi (mouse) of L-[2,3,4,5-³H]proline (Amersham) was injected intraocularly[26,36]. At 10–14 d later (cat) or 6–8 d later (mouse), animals were given an overdose of sodium pentobarbital (200 mg kg$^{-1}$ cat; 1 mg g$^{-1}$ mouse); VC was cut and frozen in M-1 mounting medium (ThermoShandon). Cryostat sections (16–25 μm) were fixed in 4% paraformaldehyde/0.1 M sodium phosphate-buffered saline (PBS), pH 7.0, washed twice in PBS and dehydrated through an ethanol series. Sections were coated with NTB-2 emulsion (Kodak) and developed after 2–3 months.

**Ocular dominance column labeling experiments in cat.** The normal pattern of *Arc* induction was compared to that of the thalamocortical projection in one adult cat and one P42 cat. *Arc* induction was done 9 d to 2 weeks after monocular [³H]proline injection (see above). Under anesthesia with inhaled isofluorane, 3 mM TTX solution (1 μl per 100 g body weight; Sigma) was injected into the eye that had received the [³H]proline injection previously. The cat was put in total darkness for 24 h and then returned to a lighted environment for 30 min in the alert condition. After light exposure, an intraperitoneal overdose of euthasol (200 mg kg$^{-1}$ to effect) was given; the brain was removed and frozen in M-1 medium.

In a second experiment, the pattern of *Arc* expression in VC was compared to that of BDNF[28]. One eye was injected with TTX (3 mM; 1 μl per 100 g body weight; Sigma) at P43 to block retinal activity. The cat was reared until P45 and euthanized; its brain was removed, frozen in M-1 medium and prepared for *in situ* hybridization. Four additional cats received MD from P32–42. Under general anesthesia with isofluorane (see above), one eye was sutured and an intraocular injection of [³H]proline was made into one eye (*n* = 2 animals, deprived eye; *n* = 2 animals, nondeprived eye). Under isofluorane anesthesia 9 d later, TTX solution was injected into the eye that had received the [³H]proline injection previously. The cat was placed in total darkness for 24 h and then returned to a lighted environment for 30 min in the alert condition. In two animals the DE was exposed to light; in the other two animals the nondeprived eye was exposed to light. Animals were euthanized and brain tissue removed as described above.

***In situ* hybridization.** The following were used as probes: full-length mouse *Arc* cDNA (gift from P. Worley, Johns Hopkins University), full-length mouse *Rorb* (RORβ) cDNA (IMAGE Consortium Clone ID5358124; Open Biosystems), mouse *c-fos* (*Fos*) cDNA (Ambion), mouse *Camk2a* and *GAD67* (*Gad1*) cDNAs (gifts from S. Nakanishi, Kyoto University), and cat *BDNF* cDNA[28]. A mouse *ER81* (*Etv1*) cDNA was obtained by RT-PCR. *In situ* hybridization was performed as described previously[28]. Images were taken using dark-field optics with a cooled CCD camera (SPOT, Diagnostic instruments), then analyzed using Photoshop, NIH Image and MATLAB software. Double *in situ* hybridization was performed as described previously[43]. Sense probes yielded only background levels of signal (data not shown).

**Quantification of *Arc* induction across multiple cortical layers.** The ratio of signal intensity of *Arc in situ* hybridization in monocular to binocular zone (**Fig. 2d**) was calculated as follows: images of *Arc in situ* hybridization were transferred to NIH image software for box scans. A box was drawn to enclose hybridization signal in layers 2–4 of the BZ in each image, and average signal intensity of *Arc in situ* hybridization in the box was calculated. Adjacent areas of cortex were scanned in similar fashion through the entire primary VC, including the MZ. Ratio of signal intensity in MZ to BZ was calculated by selecting the box with minimum value and that with maximum value. Three animals (8–12 sections) were scanned at each age.

For pairwise analyses (**Figs. 3c** and **5i**), a section from an experimental (ME or MD) animal was mounted with that from a normally reared animal on the same glass slide and processed for *in situ* hybridization simultaneously. In each pair of sections, mean signal intensity of *Arc* signal was measured in VC across all layers in V1 and V2; then relative *Arc* induction (experimental to normal) was calculated pairwise. At least 7–8 pairs of sections in 4 animals were scanned.

**Densitometric scans of *Arc* induction in specific cortical layers.** Quantitative analysis of *Arc* expression was performed in MATLAB (Mathworks) by line scans in layers 2/3, 4 or 6 (**Figs. 2e** and **4c**). At each age, 11–18 sections from three animals were scanned. Analyses were performed blind to age and manipulation; slides from different animals and manipulations were interleaved and only reassembled once decoded. For each section, a line along the center of the chosen layer was generated by selecting 20–100 points and performing a cubic spline interpolation between these points. At every pixel along this line, a perpendicular line through the layer (30–60 pixels long; 1 pixel = 1.75 μm) was computed, and the average signal intensity of pixels along this line was measured. The resulting intensity line scan was low-pass filtered (7 pt triangular), generating a curve of *Arc* signal intensity versus distance along the layer of interest. *Arc* signal rose from a minimum in both V1 and V2 to a maximum within the binocular zone (**Fig. 2e**). BZ width was measured as the region around the intensity maximum in which signal intensity was greater than 2 s.d. of the *Arc* background signal intensity (determined as average intensity of 30 pixels in the region of minimum Arc induction outside the BZ; this method would, if anything, underestimate BZ width). The area of V1 and V2 in which *Arc* induction is at a minimum is defined as the monocular zone. To quantify the strength of *Arc* induction, average signal intensity above background within the BZ was computed; normalized intensity = total signal/width of BZ, where normalized intensity was interpreted as a measure of strength of eye input. In addition, scans from each age were aligned and averaged to generate a curve of average ipsilateral eye representation (**Fig. 2f**).

**Real-time quantitative PCR analyses of *Arc* mRNA.** Measurements of *Arc* mRNA were made after 30-min light exposure in two separate experiments:

(i) in visual cortex of P34 mice monocularly deprived beginning at P18 or (ii) in visual cortex of adult mice (P96) that had received 4-d prior MD. Each experimental condition was paired with measurements from VC receiving no manipulation at the corresponding age (P34 or P96) ($n = 5$–6 mice in each condition). Mice were euthanized and brains removed. V1 and V2 were microdissected from coronal 2-mm-thick brain slices cut on an acrylic matrix (Ted Pella) and frozen immediately on dry ice. Total RNA was isolated using Trizol (Gibco-BRL). cDNA was synthesized using the iScript cDNA Synthesis Kit (Bio-Rad). Real-time PCR reactions were carried out on a SmartCycler system (Cepheid). A reaction mix contained 1× iQ SYBR Green Supermix (BioRad), 100 nM of each oligonucleotide primer and 10 ng of cDNA in 25 µl total volume. The relative amount of *Arc* was normalized to the level of internal control message, for hypoxanthine phosphoribosyltransferase (HPRT). Primers used were *Arc* forward, 5′-gaaggagtttctgcaatacagtgag-3′; *Arc* reverse, 5′-acatactgaatgatctcctcctcct-3′; HPRT (*Hprt1*) forward, 5′-tgctcgagatgtcatgaagg-3′; HPRT reverse, 5′-tatgtcccccgttgactgat-3′. Real-time PCR was performed according to the comparative threshold cycle ($C_T$) method (SmartCycler manufacturer's instructions). Differences in threshold crossing cycle between Arc and HPRT (equal to dArc) were calculated for each condition; then the levels of Arc expression were computed as $2^{-dArc}$, and ratios of Arc mRNA levels in deprived to unmanipulated cortex were computed.

*Note: Supplementary information is available on the Nature Neuroscience website.*

1. Katz, L.C. & Crowley, J.C. Development of cortical circuits: lessons from ocular dominance columns. *Nat. Rev. Neurosci.* **3**, 34–42 (2002).
2. Feller, E. & Feldman, D.E. Synaptic basis for developmental plasticity in somatosensory cortex. *Curr. Opin. Neurobiol.* **14**, 89–95 (2004).
3. Hubel, D.H., Wiesel, T.N. & LeVay, S. Plasticity of ocular dominance columns in monkey striate cortex. *Philos. Trans. R. Soc. Lond. B Biol. Sci.* **278**, 377–409 (1977).
4. Katz, L.C. & Shatz, C.J. Synaptic activity and the construction of cortical circuits. *Science* **274**, 1133–1138 (1996).
5. Crair, M.C. Neuronal activity during development: permissive or instructive? *Curr. Opin. Neurobiol.* **9**, 88–93 (1999).
6. Hensch, T.K. Controlling the critical period. *Neurosci. Res.* **47**, 17–22 (2003).
7. Gordon, J.A., Cioffi, D., Silva, A.J. & Stryker, M.P. Deficient plasticity in the primary visual cortex of alpha-calcium/calmodulin-dependent protein kinase II mutant mice. *Neuron* **17**, 491–499 (1996).
8. Hensch, T.K. *et al.* Local GABA circuit control of experience-dependent plasticity in developing visual cortex. *Science* **282**, 1504–1508 (1998).
9. Sawtell, N.B. *et al.* NMDA receptor-dependent ocular dominance plasticity in adult visual cortex. *Neuron.* **38**, 977–985 (2003).
10. Drager, U.C. Receptive fields of single cells and topography in mouse visual cortex. *J. Comp. Neurol.* **160**, 269–290 (1975).
11. Caviness, V.S., Jr. Architectonic map of neocortex of the normal mouse. *J. Comp. Neurol.* **164**, 247–263 (1975).
12. Fagiolini, M., Pizzorusso, T., Berardi, N., Domenici, L. & Maffei, L. Functional postnatal development of the rat primary visual cortex and the role of visual experience: dark rearing and monocular deprivation. *Vision Res.* **34**, 709–720 (1994).
13. Gordon, J.A. & Stryker, M.P. Experience-dependent plasticity of binocular responses in the primary visual cortex of the mouse. *J. Neurosci.* **16**, 3274–3286 (1996).
14. Antonini, A., Fagiolini, M. & Stryker, M.P. Anatomical correlates of functional plasticity in mouse visual cortex. *J. Neurosci.* **19**, 4388–4406 (1999).
15. Antonini, A. & Stryker, M.P. Rapid remodeling of axonal arbors in the visual cortex. *Science* **260**, 1819–1821 (1993).
16. Lyford, G.L. *et al.* Arc, a growth factor and activity-regulated gene, encodes a novel cytoskeleton-associated protein that is enriched in neuronal dendrites. *Neuron* **14**, 433–445 (1995).
17. Morgan, J.I. & Curran, T. Stimulus-transcription coupling in the nervous system: involvement of the inducible proto-oncogenes fos and jun. *Annu. Rev. Neurosci.* **14**, 421–451 (1991).
18. Kaczmarek, L. & Chaudhuri, A. Sensory regulation of immediate-early gene expression in mammalian visual cortex: implications for functional mapping and neural plasticity. *Brain Res. Brain Res. Rev.* **23**, 237–256 (1997).
19. Guzowski, J.F., McNaughton, B.L., Barnes, C.A. & Worley, P.F. Environment-specific expression of the immediate-early gene Arc in hippocampal neuronal ensembles. *Nat. Neurosci.* **2**, 1120–1124 (1999).
20. Schuett, S., Bonhoeffer, T. & Hubener, M. Mapping retinotopic structure in mouse visual cortex with optical imaging. *J. Neurosci.* **22**, 6549–6559 (2002).
21. Kalatsky, V.A. & Stryker, M.P. New paradigm for optical imaging: temporally encoded maps of intrinsic signal. *Neuron* **38**, 529–545 (2003).
22. Hubener, M. Mouse visual cortex. *Curr. Opin. Neurobiol.* **13**, 413–420 (2003).
23. Schaeren-Wiemers, N., Andre, E., Kapfhammer, J.P. & Becker-Andre, M. The expression pattern of the orphan nuclear receptor RORβ in the developing and adult rat nervous system suggests a role in the processing of sensory information and in circadian rhythm. *Eur. J. Neurosci.* **9**, 2687–2701 (1997).
24. Weimann, J.M. *et al.* Cortical neurons require Otx1 for the refinement of exuberant axonal projections to subcortical targets. *Neuron* **24**, 819–831 (1999).
25. Liu, X.B. & Jones, E.G. Localization of alpha type II calcium calmodulin-dependent protein kinase at glutamatergic but not gamma-aminobutyric acid (GABAergic) synapses in thalamus and cerebral cortex. *Proc. Natl. Acad. Sci. USA* **93**, 7332–7336 (1996).
26. LeVay, S., Stryker, M.P. & Shatz, C.J. Ocular dominance columns and their development in layer IV of the cat's visual cortex: a quantitative study. *J. Comp. Neurol.* **179**, 223–244 (1978).
27. Drager, U.C. Autoradiography of tritiated proline and fucose transported transneuronally from the eye to the visual cortex in pigmented and albino mice. *Brain Res.* **82**, 284–292 (1974).
28. Lein, E.S. & Shatz, C.J. Rapid regulation of brain-derived neurotrophic factor mRNA within eye-specific circuits during ocular dominance column formation. *J. Neurosci.* **20**, 1470–1483 (2000).
29. Shatz, C.J. & Stryker, M.P. Ocular dominance in layer IV of the cat's visual cortex and the effects of monocular deprivation. *J. Physiol. (Lond.)* **281**, 267–283 (1978).
30. LeVay, S., Wiesel, T.N. & Hubel, D.H. The development of ocular dominance columns in normal and visually deprived monkeys. *J. Comp. Neurol.* **191**, 1–51 (1980).
31. Crair, M.C., Horton, J.C., Antonini, A. & Stryker, M.P. Emergence of ocular dominance columns in cat visual cortex by 2 weeks of age. *J. Comp. Neurol.* **430**, 235–249 (2001).
32. Kageyama, G.H. & Robertson, R.T. Development of geniculocortical projections to visual cortex in rat: evidence early ingrowth and synaptogenesis. *J. Comp. Neurol.* **335**, 123–148 (1993).
33. Godement, P., Salaun, J. & Imbert, M. Prenatal and postnatal development of retinogeniculate and retinocollicular projections in the mouse. *J. Comp. Neurol.* **230**, 552–575 (1984).
34. Muir-Robinson, G., Hwang, B.J. & Feller, M.B. Retinogeniculate axons undergo eye-specific segregation in the absence of eye-specific layers. *J. Neurosci.* **22**, 5259–5264 (2002).
35. Pham, T.A., Rubenstein, J.L., Silva, A.J., Storm, D.R. & Stryker, M.P. The CRE/CREB pathway is transiently expressed in thalamic circuit development and contributes to refinement of retinogeniculate axons. *Neuron* **31**, 409–420 (2001).
36. Drager, U.C. Observations on monocular deprivation in mice. *J. Neurophysiol.* **41**, 28–42 (1978).
37. Porciatti, V., Pizzorusso, T. & Maffei, L. The visual physiology of the wild type mouse determined with pattern VEPs. *Vision Res.* **39**, 3071–3081 (1999).
38. Pizzorusso, T. *et al.* Reactivation of ocular dominance plasticity in the adult visual cortex. *Science* **298**, 1248–1251 (2002).
39. Hubel, D.H. & Wiesel, T.N. The period of susceptibility to the physiological effects of unilateral eye closure in kittens. *J. Physiol. (Lond.)* **206**, 419–436 (1970).
40. Pham, T.A. *et al.* A semi-persistent adult ocular dominance plasticity in visual cortex is stabilized by activated CREB. *Learn. Mem.* **11**, 1–10 (2004).
41. Desai, N.S., Cudmore, R.H., Nelson, S.B. & Turrigiano, G.G. Critical periods for experience-dependent synaptic scaling in visual cortex. *Nat. Neurosci.* **5**, 783–789 (2002).
42. Turrigiano, G.G & Nelson, S.B. Homeostatic plasticity in the developing nervous system. *Nat. Rev. Neurosci.* **5**, 97–107 (2004).
43. Kaneko, S. *et al.* Synaptic integration mediated by striatal cholinergic interneurons in basal ganglia function. *Science* **289**, 633–637 (2000).